

# UCSF

## UC San Francisco Previously Published Works

### Title

Premetastatic soil and prevention of breast cancer brain metastasis

### Permalink

<https://escholarship.org/uc/item/3zs4146r>

### Journal

Neuro-Oncology, 15(7)

### ISSN

1522-8517

### Authors

Liu, Yan  
Kosaka, Akemi  
Ikeura, Maki  
et al.

### Publication Date

2013-07-01

### DOI

10.1093/neuonc/not031

Peer reviewed

# Premetastatic soil and prevention of breast cancer brain metastasis

Yan Liu, Akemi Kosaka, Maki Ikeura, Gary Kohanbash, Wendy Fellows-Mayle, Linda A. Snyder, and Hideho Okada

*Brain Tumor Program (Y.L., A.K., M.I., G.K., H.O.) and Surgical Oncology, University of Pittsburgh Cancer Institute, Pittsburgh, Pennsylvania (H.O.); Department of Neurological Surgery, University of Pittsburgh School of Medicine, Pittsburgh, Pennsylvania (Y.L., A.K., W.F.-M., H.O.); Department of Surgery, University of Pittsburgh School of Medicine, Pittsburgh, Pennsylvania (H.O.); Department of Immunology, University of Pittsburgh School of Medicine, Pittsburgh, Pennsylvania (H.O.); Department of Infectious Diseases and Microbiology, University of Pittsburgh Graduate School of Public Health, Pittsburgh, Pennsylvania (G.K.); Janssen Research and Development, LLC, Spring House, Pennsylvania (L.A.S.)*

**Background.** As therapies for systemic cancer improve and patients survive longer, the risk for brain metastases increases. We evaluated whether immune mechanisms are involved in the development of brain metastasis.

**Methods.** We conducted our studies using BALB/c mice bearing syngeneic 4T1 mammary adenocarcinoma cells in the mammary gland.

**Results.** The brains of mice bearing 4T1 tumors at day 14 had no detectable metastatic tumor cells but presented with marked accumulation of bone marrow–derived CD11b<sup>+</sup>Gr1<sup>+</sup> myeloid cells, which express high levels of inflammatory chemokines S100A8 and S100A9. In vitro, S100A9 attracts 4T1 cells through Toll-like receptor 4 and CD11b<sup>+</sup>Gr1<sup>+</sup> myeloid cells through Toll-like receptor 4 and the receptor for advanced glycation end-products. Systemic treatment of 4T1-bearing mice with anti-Gr1 (RB6-8C5) monoclonal antibody reduces accumulation of CD11b<sup>+</sup>Gr1<sup>+</sup> myeloid cells in the day-14 premetastatic brain as well as subsequent brain metastasis of 4T1 cells detected on day 30. Furthermore, treatment of 4T1 tumor-bearing mice with the cyclooxygenase-2 inhibitor celecoxib or genetic disruption of cyclooxygenase-2 in 4T1 cells inhibits the inflammatory chemokines and infiltration of CD11b<sup>+</sup>Gr1<sup>+</sup> myeloid cells in the premetastatic brain and subsequent formation of brain metastasis.

**Conclusions.** Our results suggest that the primary tumor induces accumulation of CD11b<sup>+</sup>Gr1<sup>+</sup> myeloid cells in the brain to form “premetastatic soil” and inflammation

mediators, such as S100A9, that attract additional myeloid cells as well as metastatic tumor cells. Celecoxib and anti-Gr1 treatment may be useful for blockade of these processes, thereby preventing brain metastasis in patients with breast cancer.

**Keywords:** brain metastasis, breast cancer, CCL2, myeloid-derived suppressor cells, prostaglandin-E<sub>2</sub>, S100A8/A9.

**B**reast cancer is the most common malignancy in women in the United States, and metastasis is a major cause of morbidity and mortality. About 15%–20% of women with metastatic breast cancer experience clinically symptomatic metastases to the brain,<sup>1,2</sup> while at autopsy, brain metastases are in fact discovered in more than 30% of breast cancer patients.<sup>2,3</sup> The incidence of brain metastases has been increasing as treatment options for primary breast cancer improve and patients live longer. Unfortunately, we lack effective treatment options: although stereotactic radiosurgery has emerged as a possible alternative to whole-brain radiotherapy and surgery,<sup>4</sup> the median overall survival for patients with breast cancer metastases to the brain remains <1 year.<sup>5</sup>

Cancer metastasis depends on the conditions of both the organ in which the primary tumor originates and the tissue to which the tumor cells travel.<sup>6</sup> Recent studies have suggested that the primary tumor can immunologically condition the metastatic site to facilitate its metastatic spread.<sup>7</sup> Tumor-associated host cells, such as myeloid cells, appear to mediate the conditioning in the metastatic site.<sup>8</sup> However, it remains unclear whether the primary breast cancer impacts the environment of the brain, thereby promoting brain metastasis.

Received November 5, 2012; accepted February 8, 2013.

**Corresponding Author:** Hideho Okada, MD, PhD, 1.19e Research Pavilion at the Hillman Cancer Center, 5117 Centre Ave. Pittsburgh, PA, 15213-1863 (okadah@upmc.edu).

In the current study, we used BALB/c mice and the syngeneic 4T1 mammary carcinoma model.<sup>9</sup> This tumor model shares many features with human breast cancer in terms of progressive growth in the mammary gland and active metastasis to other organs, while the model is virtually nonimmunogenic in syngeneic mice.<sup>9</sup> Our data indicate for the first time that primary breast cancer creates premetastatic soils in the brain via inflammatory mediators and CD11b<sup>+</sup>Gr1<sup>+</sup> myeloid cells, thereby promoting brain metastasis.

## Materials and Methods

### Cell Lines and Animals

4T1 cells, 4T1 cells transfected with enhanced green fluorescent protein (4T1-EGFP), and JC mammary adenocarcinoma cell lines (H-2<sup>d</sup>) were cultured in RPMI-1640 (Roswell Park Memorial Institute medium; Mediatech) and supplemented with 10% fetal bovine serum (Gemini Bio-Products) and 1% penicillin/streptomycin (Invitrogen). H-2<sup>d</sup> BALB/c mice were obtained from the Jackson Laboratory. EGFP transgenic BALB/c mice were kindly provided by Dr Stephen H. Thorne (University of Pittsburgh). Animals were handled in the Animal Facility at the University of Pittsburgh per an Institutional Care and Use Committee–approved protocol.

### Quantitative Real-time PCR

The procedure has been described previously.<sup>10</sup> The following primers and probes were obtained from Applied Biosystems: *CCL2* (Mm00441242\_m1), *CCL17* (Mm01244826\_g1), *CCL22* (Mm00436439\_m1), *CCL28* (Mm00445039\_m1), *COX2* (Mm03294838\_g1), *CSF-1* (Mm01200006\_m1), *CXCL12* (Mm00445553\_m1), *S100A8* (Mm00496696\_g1), *S100A9* (Mm00656925\_m1), *SAA3* (Mm00441203\_m1), and *GAPDH* (Mm99999915\_g1). *GAPDH* was used as the internal control.

### Isolation of Brain-Infiltrating Leukocytes

The procedure to isolate brain-infiltrating leukocytes (BILs) has been described previously.<sup>10–12</sup> BILs were pooled from 3 or 5 mice in a given group, and leukocyte-gated populations were evaluated using an Accuri C6 flow cytometer (Becton Dickinson). Fluorescein isothiocyanate–conjugated anti-Ly6C, phycoerythrin-conjugated anti-Ly6G, phycoerythrin-conjugated anti-Gr1, and allophycocyanin-conjugated anti-CD11b were purchased from eBioscience. Sorting was performed using a MoFlo high-speed cell sorter (Beckman Coulter).

### Establishment of the EGFP Bone Marrow Chimera Mouse Model

Bone marrow (BM) transplantation was performed with EGFP transgenic BALB/c mice as donors and BALB/c

mice as recipients. Prior to transplantation, the recipient mice received 10 Gy irradiation. Twenty-four hours after irradiation, the mice were transplanted with  $1 \times 10^6$  BM cells from the donor mice by i.v. injection in the tail vein. After 2 weeks, peripheral blood cells were collected from the recipient mice and analyzed using flow cytometry to confirm the chimerism with donor-derived cells.

### Fluorescence Imaging of Brain Tissues

Mice bearing 4T1-EGFP cells in the primary mammary gland were sacrificed and perfused with 2% paraformaldehyde. The brain was removed and cut into 3-mm-thick slices using mouse brain matrix (Kent Scientific) and blades. Imaging was performed under Multiphoton Fluorescence Microscopy (Olympus) at the Cell and Tissue Imaging Facility within the Center for Biological Imaging of the University of Pittsburgh.

### Live Animal Imaging

Imaging was performed using an IVIS200 Imaging System (Xenogen Biosciences) at the In Vivo Imaging Facility of the University of Pittsburgh Cancer Institute. Mice were anesthetized using isoflurane.

### Clonogenic Assay for Evaluation of Spontaneous Brain Metastasis

The procedure has been described previously<sup>13</sup> and performed with minor modifications. In brief, BALB/c mice first received inoculations of  $5 \times 10^4$  tumor cells in the primary mammary gland. On day 14 or 30, mice were sacrificed and perfused with 20 mL phosphate buffered saline (PBS). Their brains were removed and finely minced with 18G and 27G needles. After extensive washing with PBS, single cell suspensions from each mouse were plated in a 10-cm tissue culture dish. The cells were cultured in the presence of 60  $\mu$ M 6-thioguanine (Sigma-Aldrich) during the final 7–10 days of the total 28-day culture period to selectively grow tumor cells. The culture dishes were then fixed with methanol and stained with crystal violet for counting the foci of tumor cells that gave rise from each animal.

### Histidine-fused S100A9 and Anti-S100A9 Antibody

Histidine (His)-fused recombinant murine S100A9 protein (*His-fusion S100A9* plasmid was kindly provided by Dr Yoshiro Maru, Tokyo Women's Medical University) and anti-S100A9 polyclonal antibody (Ab) were generated by Biomatik. For Ab production, New Zealand rabbits were immunized with recombinant S100A9-His protein with 8 boosts over ~70 days. Serum from the rabbits was purified by protein A/G affinity column. Control histamine and rabbit immunoglobulin (Ig)G were purchased from Sigma-Aldrich.

### *In vitro Migration Assay*

Migration of 4T1 tumor cells and BM-derived CD11b<sup>+</sup> cells to recombinant S100A9-His protein was evaluated using a chemotaxis Boyden chamber (Neuro Probe). The upper and lower wells were separated by a 5- $\mu$ m pore-size polyvinylpyrrolidone-free polycarbonate membrane (Nucleopore). Recombinant S100A9-His at gradient concentrations was applied to the lower wells. Aliquots of cell suspensions ( $5 \times 10^4$  cells/100  $\mu$ L/well) were seeded in each of the upper wells and incubated for 3 h at 37°C with 5% CO<sub>2</sub>. Anti-Toll-like receptor 4 (TLR4) and anti-receptor for advanced glycation end-products (RAGE) blocking Abs were purchased from eBioscience and Abcam, respectively. The carboxylated N-glycan-specific monoclonal (m)Ab GB3.1 and control isotype Ab were kindly provided by Dr Geetha Srikrishna (Sanford Children's Health Research Center, Sanford-Burnham Medical Research Institute).

### *Ab Treatment*

BALB/c mice bearing 4T1 tumor cells received Ab treatments via i.p. injections on days 3, 7, 10, and 14 at the following doses: anti-Gr1 Ab (clone RB6-8C5, 0.25 mg/dose) or control IgG, anti-mouse chemokine C-C ligand 2 (CCL2) mAb (C1142, 0.2 mg/dose; Janssen), or control isotype Ab (cVaM; Janssen). The heavy chains and light chains in cVaM were derived from 2 different mouse Abs that recognize other antigens. The cVaM Ab does not recognize either antigen, unlike the parental Abs.

### *Celecoxib Treatment*

BALB/c mice bearing 4T1 tumors received celecoxib (Celebrex, Pfizer) via diet (6 mg/day) from day 1 to day 14 (for evaluation of premetastatic conditions) or to day 30 (for evaluation of spontaneous metastases).

### *Cyclooxygenase-2 Knockdown in 4T1 cells*

Cultured 4T1 cells were transfected with cyclooxygenase (COX)2-targeting short hairpin RNA or nontargeting short hairpin RNA control (OriGene) using Lipofectamine 2000 (Invitrogen) according to the manufacturer's instructions, followed by selection of stable transfectant clones with 10  $\mu$ g/mL puromycin. The targeting sequence for COX2 was 5'-CTGGTGCC TGGTCTGATGATGTATGCCAC-3'. The clone that showed the most efficient reduction of COX2 without affecting in vitro growth, based on COX2 PCR and prostaglandin-E<sub>2</sub> (PGE<sub>2</sub>) enzyme-linked immunosorbent assay, was selected and used in the current study.

### *Statistical Analysis*

Paired or unpaired data indicated as mean  $\pm$  SD were analyzed using a paired or nonpaired, respectively, Student's *t*-test. *P* < .05 was considered significant.

## Results

### *Mice Bearing 4T1 Tumors in the Mammary Gland Present Accumulation of CD11b<sup>+</sup>Gr1<sup>+</sup> Cells and Upregulation of Inflammatory Chemokines in the Premetastatic Brain*

We first evaluated the time course of spontaneous metastasis to the brain using BALB/c mice bearing 4T1 tumors. On day 14 following the inoculation of the tumor cells in the mammary gland, neither clonogenic assays (Fig. 1A) nor microscopic analyses using 4T1-EGFP cells (Fig. 1B) demonstrated any evidence of tumor cell metastasis in the brain, while these assays readily detected metastatic tumor cells in the brains of mice bearing 4T1 tumors at day 30. Furthermore, we performed additional experiments with 4T1 tumor cells stably transduced with luciferase (4T1-*luc*) and PCR for specific primers for luciferase. We readily detected luciferase mRNA in day-30 brains but not in day-14 brains (data not shown).

However, when the brains of mice bearing 4T1 tumors of day 14 were evaluated for BILs and mRNA expression for inflammatory chemokines, there was a marked accumulation of CD11b<sup>+</sup>Gr1<sup>+</sup>, CD11b<sup>+</sup>Ly6C<sup>+</sup>, and CD11b<sup>+</sup>Ly6G<sup>+</sup> immature myeloid cells (IMCs) (Fig. 1C) and upregulation of *S100A8*, *S100A9*, *SAA3*, and *CCL2* (Fig. 1D) compared with non-tumor-bearing control mice. Other chemokines that are often described for their roles in cancer-induced immunosuppression (namely, *CCL17*, *CCL22*,<sup>14</sup> *CCL28*,<sup>15</sup> *CXCL12*,<sup>16</sup> and *CSF-1*<sup>17</sup>) were not significantly elevated in the mice bearing day-14 tumors. Based on the absence of metastatic tumor cells despite the highly inflammatory conditions, we hereby term the brain of mice bearing 4T1 tumors of day 14 as the premetastatic brain.

### *CD11b<sup>+</sup>Gr1<sup>+</sup> Cells That Accumulated in the Premetastatic Brain Are Bone Marrow Derived and Responsible for the Brain Metastasis of 4T1 Tumor Cells*

Of the 2 CD11b<sup>+</sup> myeloid cell populations in the brain, resident microglia are long-standing brain resident cells, while BM-derived myeloid cells have recently migrated in the brain from the systemic circulation.<sup>18</sup> To determine whether the IMCs that accumulated in the brains of 4T1-bearing mice were BM derived, we established BM chimera mice in whom BM cells were replaced with cells from EGFP-transgenic mice. As demonstrated in Fig. 2A, in vivo imaging of EGFP<sup>+</sup> cells in mice bearing day-14 mammary 4T1 tumors demonstrated positive EGFP signals in the head, while control non-tumor-bearing mice did not show detectable signals. Indeed, flow cytometric analysis of BILs (Fig. 2B) revealed the enhanced accumulation of EGFP<sup>+</sup> CD11b<sup>+</sup> BILs compared with control mice.

To address whether the BM-derived IMCs were directly responsible for the formation of brain metastasis, we treated 4T1-bearing mice with anti-Gr1 mAb (RB6-8C5). We have previously demonstrated that i.p. injections of this mAb efficiently deplete

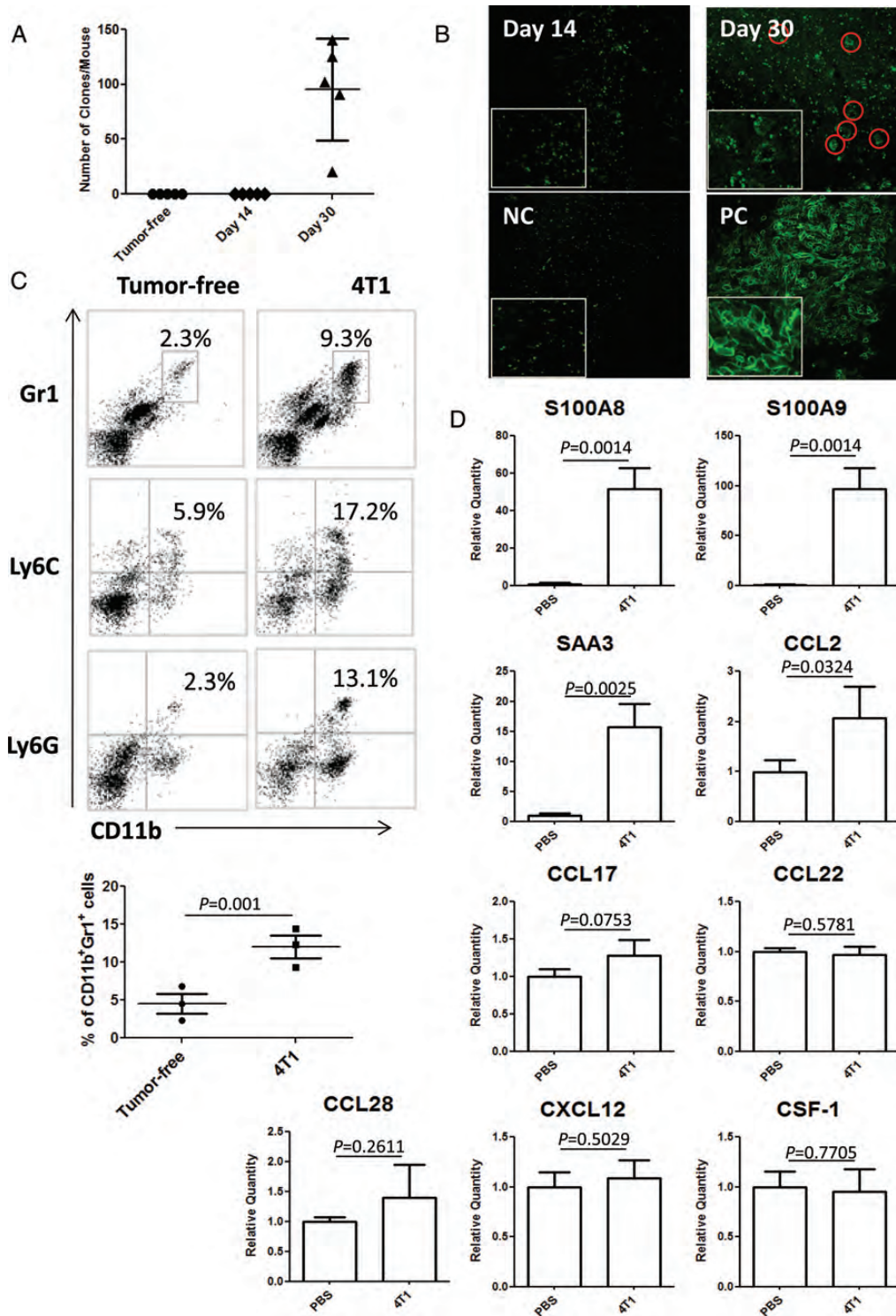


Fig. 1. The primary 4T1 tumor induces accumulation of IMCs and upregulation of inflammatory chemokines in the premetastatic brain. (A) Clonogenic assay with mice bearing 4T1 tumors of day 14 or day 30. Numbers of 4T1 cell colonies/mouse are plotted ( $n = 5$ /group). (B) Multiphoton microscopy on brain tissues from mice bearing 4T1-EGFP tumors of day 14 or day 30. NC = negative control mice without tumor inoculation. PC = positive control mice that received intracranial injection of 4T1-EGFP tumor cells. Original magnification:  $20\times$ . (C) BIL analysis on  $CD11b^+Gr1^+$ ,  $CD11b^+Ly6C^+$ , and  $CD11b^+Ly6G^+$  cells ( $n = 5$ /group). The number in each histogram indicates the percentage of double-positive cells (upper panels). The lower graph shows the percentage of  $CD11b^+Gr1^+$  cells in 3 independent experiments. Bars indicate mean  $\pm$  SD. (D) mRNA expression levels for indicated chemokines ( $n = 5$ /group) in mice bearing day-14 tumors relative to those in control mice receiving saline.

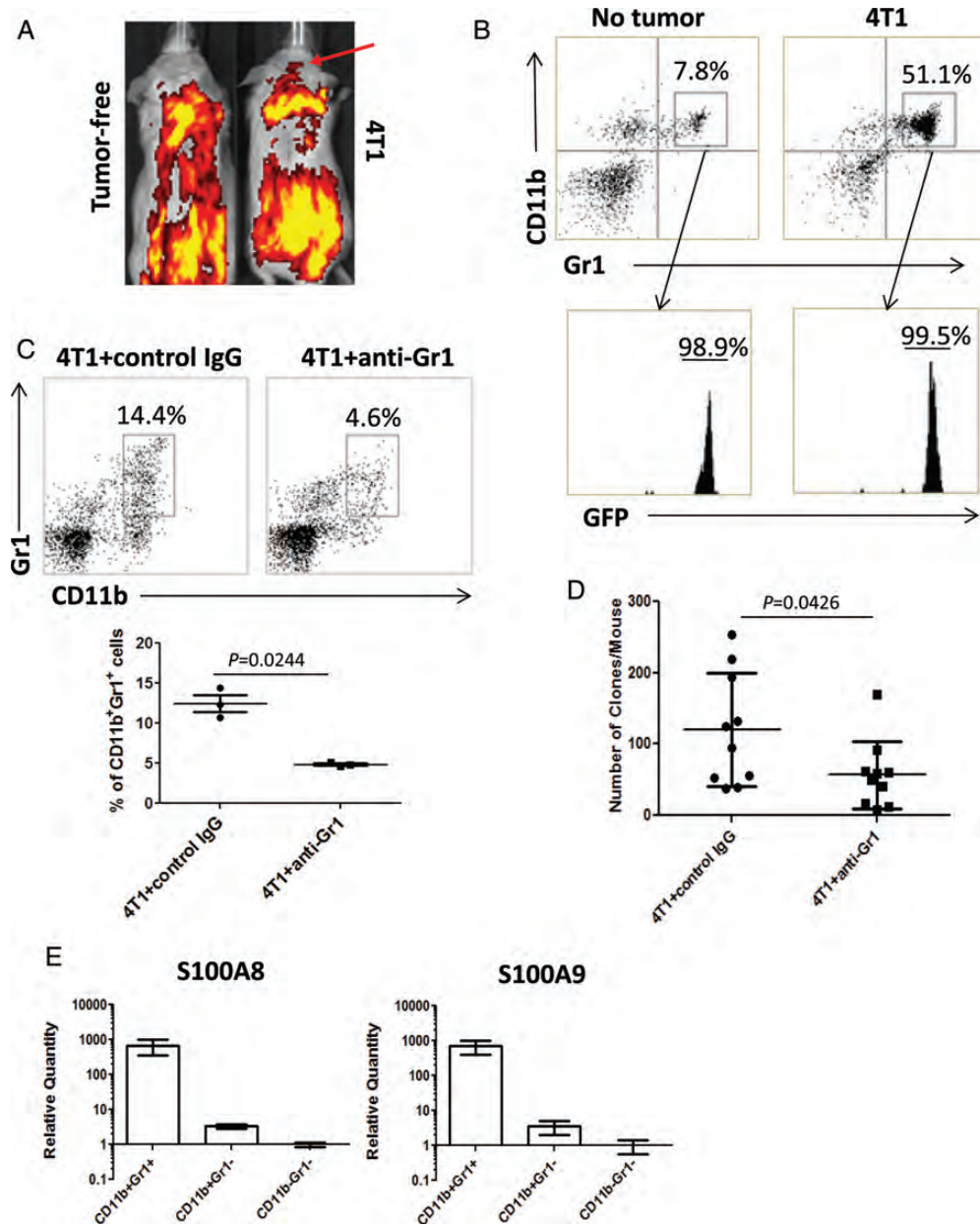


Fig. 2. BM-derived IMCs promote brain metastasis. (A and B) Mice chimeric with EGFP<sup>+</sup> BM cells with or without 4T1 tumors. (A) In vivo imaging of EGFP signals on day 14 after 4T1 cell (right) or control saline (left) injection. (B) CD11b<sup>+</sup>Gr1<sup>+</sup> BILs in tumor-free (left) or 4T1-bearing (right) mice on day 14. CD11b<sup>+</sup>Gr1<sup>+</sup> BILs were EGFP<sup>+</sup> (bottom panels). (C and D) Mice bearing 4T1 tumors were treated with anti-Gr1 mAb or control IgG. (C) CD11b<sup>+</sup>Gr1<sup>+</sup> BILs in mice treated with control IgG (left) or with anti-Gr1 mAb (right) on day 14 ( $n = 5$ /group). The number in each histogram indicates the percentage of CD11b<sup>+</sup>Gr1<sup>+</sup> cells (upper panels). The graph shows the percentage of CD11b<sup>+</sup>Gr1<sup>+</sup> cells in 3 repeated experiments. (D) Clonogenic assays with the brains of mice bearing 4T1 tumors of day 30 treated with anti-Gr1 mAb or control IgG ( $n = 10$ /group). (E) CD11b<sup>+</sup>Gr1<sup>+</sup>, CD11b<sup>+</sup>Gr1<sup>-</sup>, and CD11b<sup>-</sup>Gr1<sup>-</sup> populations of the day-14 BILs were evaluated for expression levels of *S100A8* and *S100A9* by real-time PCR (7 mice). Boxes and bars indicate range of mean values in 2 independent experiments.

CD11b<sup>+</sup>Gr1<sup>+</sup> IMCs systemically and in the microenvironment of mouse gliomas.<sup>11,12</sup> As shown in Fig. 2C, the anti-Gr1 mAb reduced CD11b<sup>+</sup>Gr1<sup>+</sup> BILs in the brains of mice bearing day-14 mammary 4T1 tumors. Furthermore, the treatment significantly reduced numbers of brain metastases based on the clonogenic assay:  $56.6 \pm 15.1$  colonies/mouse (mean  $\pm$  SD) compared with  $120.2 \pm 24.95$  colonies/mouse observed with control IgG treatment (Fig. 2D). These results

provide evidence that CD11b<sup>+</sup>Gr1<sup>+</sup> IMCs contribute to the spontaneous brain metastasis of 4T1 tumors.

#### *S100A9* Attracts CD11b<sup>+</sup>Gr1<sup>+</sup> BM Cells and 4T1 Tumor Cells via Its Cognate Receptors

As demonstrated in Fig. 1D, *S100A8* and *S100A9* (henceforth *S100A8/A9*) were 2 of the most significantly upregulated chemokines in the premetastatic brain, which

was also infiltrated by large numbers of BM-derived CD11b<sup>+</sup>Gr1<sup>+</sup> cells. Therefore, we hypothesized that CD11b<sup>+</sup>Gr1<sup>+</sup> cells would express high levels of S100A8/A9. Indeed, as shown in Fig. 2E, CD11b<sup>+</sup>Gr1<sup>+</sup> populations expressed more than 2 log scales higher levels of S100A8/A9 compared with CD11b<sup>+</sup>Gr1<sup>-</sup> and CD11b<sup>-</sup>Gr1<sup>-</sup> subpopulations of BILs.

To evaluate the role of S100A8/A9 in the observed accumulation of CD11b<sup>+</sup>Gr1<sup>+</sup> BILs and tumor cell metastasis, we produced His-fused murine S100A9 protein (S100A9-His) and anti-S100A9 polyclonal Ab. As S100A9 has a higher binding capacity to endothelial cells compared with S100A8<sup>19</sup> and plays a predominant role in leukocyte trafficking,<sup>20</sup> we prioritized our assessment on the role of S100A9 in inducing migratory activities of 4T1 tumor and BM-derived CD11b<sup>+</sup> myeloid cells, which were also Ly6C<sup>+</sup>Ly6G<sup>+</sup> (Supplementary Fig. S4). Migration of 4T1 cells toward S100A9-His took place in the range of 10 pg/mL to 10 ng/mL, maximally at 100 pg/mL (Fig. 3A). Migration of CD11b<sup>+</sup> cells was induced as low as 0.1 pg/mL S100A9-His, with the maximal migration rate observed at 1 pg/mL

(Fig. 3B). When anti-S100A9 blocking Ab was added to the lower chambers, the migration activities of 4T1 tumor cells and CD11b<sup>+</sup> cells were inhibited (Fig. 3D and E).

TLR4,<sup>21</sup> RAGE,<sup>22,23</sup> and carboxylated N-glycans<sup>24</sup> are known to be the receptors for S100A8/A9. BM-derived CD11b<sup>+</sup>Gr1<sup>+</sup> cells expressed both TLR4 and RAGE on their surface, while 4T1 cells expressed TLR4 but not RAGE (Fig. 3C). Pretreatment of 4T1 cells with anti-TLR4 mAb (Fig. 3D) or CD11b<sup>+</sup> cells with anti-TLR4, anti-RAGE, or the carboxylated N-glycan-specific mAb GB3.1 (Fig. 3E) inhibited their migration to S100A9.

*COX2 and PGE<sub>2</sub> Produced by the Primary Tumor Contribute to the Infiltration of CD11b<sup>+</sup>Gr1<sup>+</sup> Cells in the Premetastatic Brain and Spontaneous Brain Metastasis*

PGE<sub>2</sub>, an important mediator of inflammation and a metabolite of COX and PGE synthase, is highly elevated in epithelial malignancies, including breast cancer, with

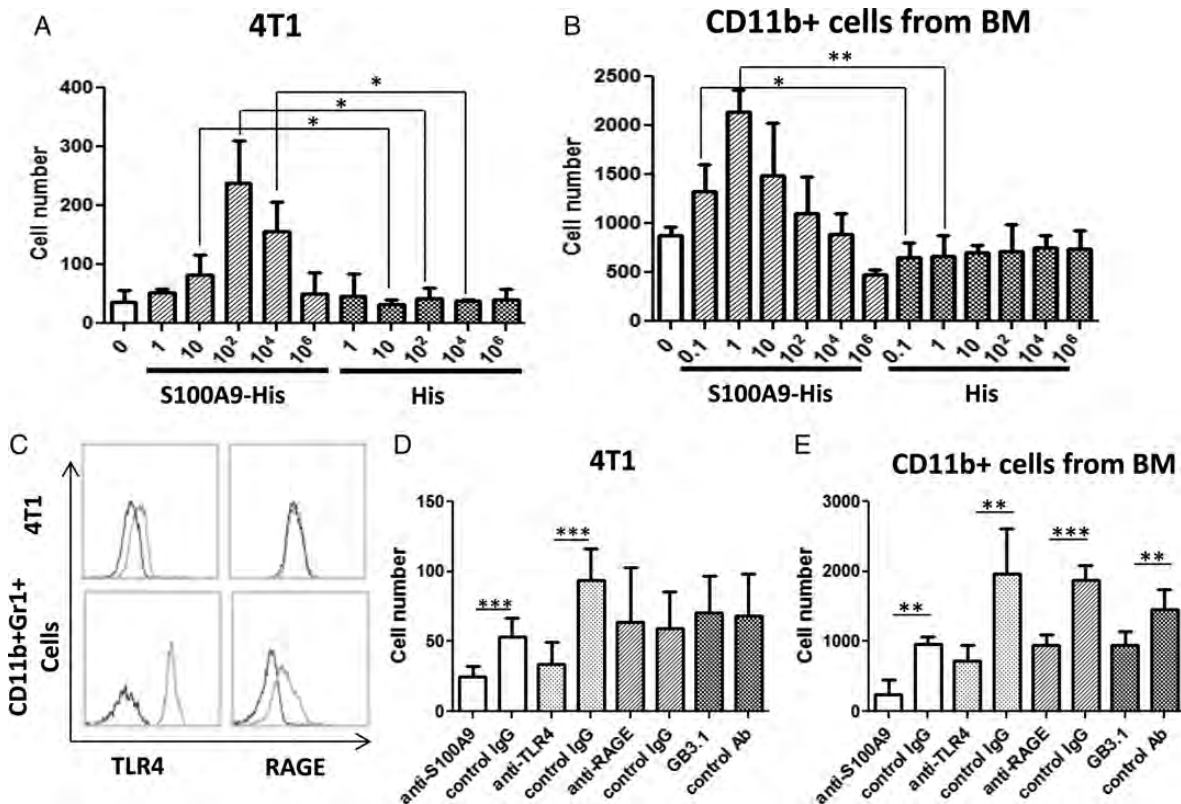


Fig. 3. S100A9 induces migration of 4T1 tumor and CD11b<sup>+</sup> myeloid cells. (A) In vitro migration of 4T1 cells induced by recombinant S100A9 at serial concentrations (pg/mL, n = 3/group). (B) In vitro migration of BM-derived CD11b<sup>+</sup> myeloid cells induced by S100A9 at serial concentrations (pg/mL, n = 3/group). (C) Expression of TLR4 and RAGE on 4T1 cells and CD11b<sup>+</sup>Gr1<sup>+</sup> splenocytes. Dotted lines indicate staining with anti-TLR4 (left panels) or anti-RAGE (right panels) mAbs. Solid lines indicate staining with isotype control IgG. (D) In vitro migration of 4T1 cells was induced by S100A9-His at 100 pg/mL. To determine the blocking effect of anti-S100A9 mAb, 1 μg/mL anti-S100A9 or its control IgG was added to the lower chamber. To determine the blocking effect of anti-TLR4, anti-RAGE, or GB3.1, 5 × 10<sup>5</sup> 4T1 cells were pre-incubated with each of these Abs (1 μg/mL) or control isotype IgG at 37°C for 20 min, before the migration assay (n = 6/group). (E) In vitro migration of CD11b<sup>+</sup> cells was induced by S100A9-His at 1 pg/mL. The methods to block CD11b<sup>+</sup> cell migration toward S100A9 using anti-S100A9, anti-TLR4, anti-RAGE, or GB3.1 are mentioned in the text. (A–E) P-values \* < .05, \*\* < .01, and \*\*\* < .001, respectively.

poor prognosis.<sup>25</sup> We addressed the role of COX2 and PGE<sub>2</sub> in our model by genetically disrupting the COX2 (and resulting PGE<sub>2</sub>; Fig. 4A) expression in 4T1 cells by stable transfection of COX2—targeting small interfering RNA (4T1-COX2 KO cells). In vivo, mice inoculated with 4T1-COX2 KO cells showed decreased percentages of both CD11b<sup>+</sup>Ly6C<sup>+</sup> and CD11b<sup>+</sup>Ly6G<sup>+</sup> IMCs in the premetastatic brain compared with mice bearing mock-transfected 4T1 cells (Fig. 4B). Mice bearing 4T1-COX2 KO also exhibited a trend toward reduced degrees of brain metastasis based on the clonogenic assay (Fig. 4;  $P = .0621$ ). These results suggest a role for COX2-PGE<sub>2</sub> synthesis by the primary tumor in the brain metastasis of 4T1 tumors.

#### Celecoxib Blocks the Upregulation of Inflammatory Chemokines, IMC Accumulation, and Brain Metastasis of 4T1 Tumors

To extend the previously discussed observations to a more clinically applicable approach, we evaluated the effects of celecoxib, a COX2 inhibitor. Oral celecoxib administration (6 mg/day) was effective to reduce CD11b<sup>+</sup>Gr1<sup>+</sup> BILs in the premetastatic brain (Fig. 5A) and expression levels of S100A8, S100A9, serum amyloid A (SAA)3, and CCL2 (Fig. 5B). Furthermore, as shown in Fig. 5C, oral celecoxib treatment significantly reduced metastasis formation ( $6.2 \pm 2.3$  colonies/mouse) compared with the control saline treatment ( $95.6 \pm 20.8$  colonies/mouse).

#### Nonmetastatic JC Mammary Adenocarcinoma Cells Produce Low Levels of PGE<sub>2</sub> and Fail to Induce Premetastatic Conditions in the Brain

To confirm the role of PGE<sub>2</sub> production by mammary carcinoma cells, we performed additional experiments

using the JC mammary adenocarcinoma, which is a BALB/c-background, weakly immunogenic, but nonmetastatic model of breast cancer.<sup>26–28</sup> JC cells produced much lower levels of PGE<sub>2</sub> in vitro compared with 4T1 cells (Supplementary Fig. S1A). Furthermore, in a striking contrast to the 4T1 model, JC cells inoculated in the mammary pad did not induce upregulation of S100A8/A9, SAA3, or CCL2 in the brain (Supplementary Fig. S1B). These findings support our conclusion that PGE<sub>2</sub> produced by the primary tumor contributes to premetastatic conditioning in the brain.

#### Treatment With Anti-CCL2 mAb Reduced the Accumulation of IMCs and the Expression of S100A8, S100A9, and SAA3 in the Premetastatic Brain

On the basis of the finding that celecoxib treatment abrogated the elevated CCL2 expression in the premetastatic brain, we sought to determine whether CCL2 would have direct contributions to the recruitment of CD11b<sup>+</sup>Gr1<sup>+</sup> cells via CCL2-CCR2.<sup>29,30</sup> I.p. administration of anti-CCL2 mAb resulted in a trend toward reduced percentage of CD11b<sup>+</sup>Gr1<sup>+</sup>, CD11b<sup>+</sup>Ly6C<sup>+</sup>, and CD11b<sup>+</sup>Ly6G<sup>+</sup> cells by ~25% (Fig. 6A) and expression levels of S100A8/A9 and SAA3 in the premetastatic brain (Fig. 6B).

#### The Liver and the Lung of Mice Bearing 4T1 Tumors of Day 14 Also Demonstrated Metastases, Increased CD11b<sup>+</sup>Gr1<sup>+</sup> Cell Infiltration, and Upregulation of S100A8/A9, SAA3, and CCL2

Although our primary focus was on the evaluation of brain metastasis, mice bearing 4T1 tumors in the mammary pad developed systemic metastases, including those of the lung and liver, and died at around day 35 after tumor inoculation, mostly of lung metastases.

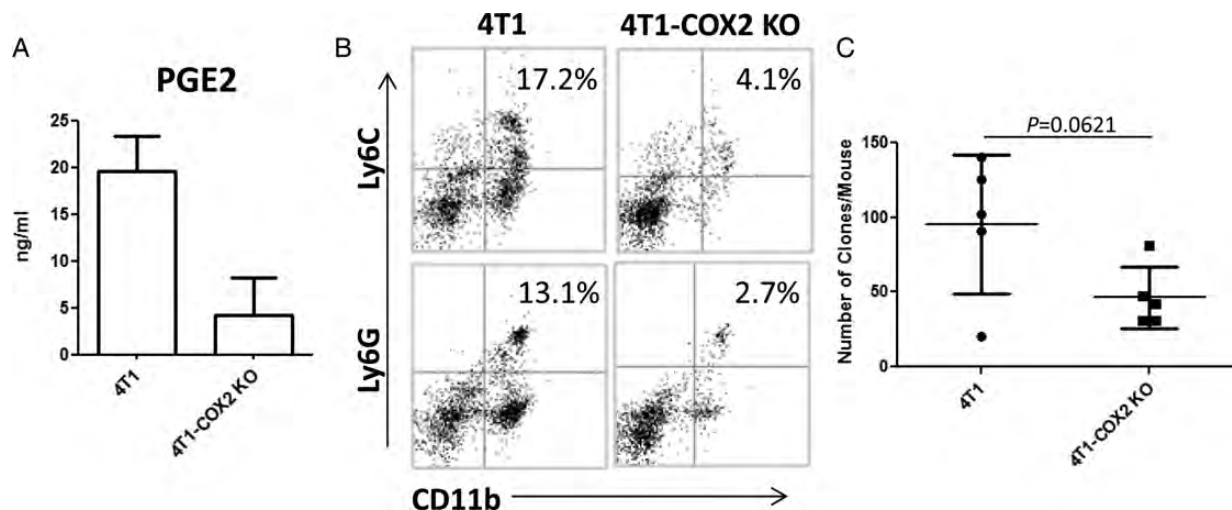


Fig. 4. PGE<sub>2</sub> produced from primary tumor induces IMC infiltration in the premetastatic brain. (A) PGE<sub>2</sub> production by mock-transfected 4T1 or 4T1-COX2 KO cells by enzyme-linked immunosorbent assay. (B) CD11b<sup>+</sup>Ly6C<sup>+</sup> and CD11b<sup>+</sup>Ly6G<sup>+</sup> BILs in mice bearing day-14 mock-transfected 4T1 or 4T1-COX2 KO tumors. BILs were pooled for each group and evaluated by flow cytometry ( $n = 5$ /group). The number in the right upper quadrant indicates the percentage of double-positive cells. (C) Clonogenic assay with mice bearing day-30 mock-transfected 4T1 or 4T1-COX2 KO tumors ( $n = 5$ /group).



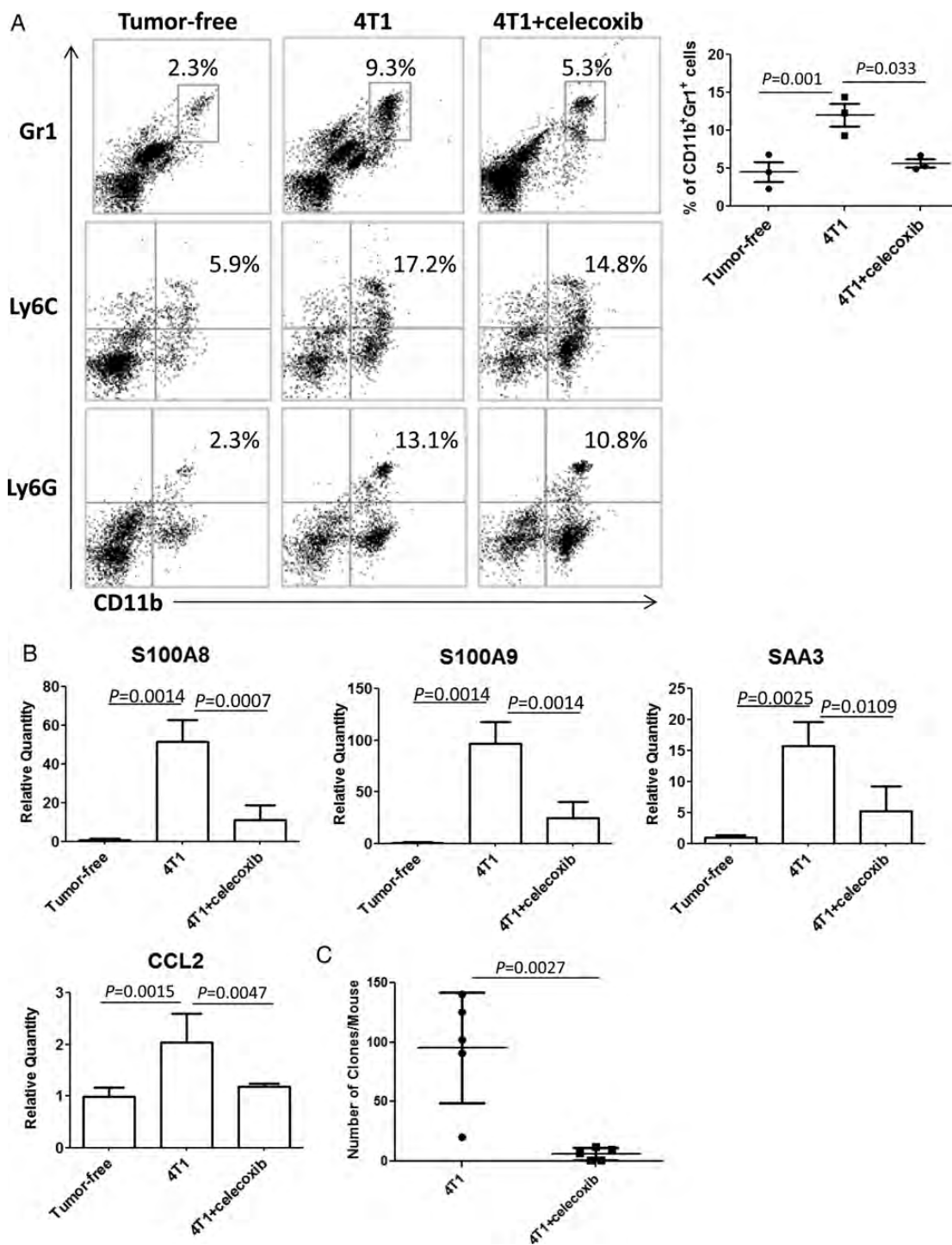


Fig. 5. Systemic administration of celecoxib reduces infiltration of IMCs, inflammatory chemokines, and tumor metastasis in the brain. (A) CD11b<sup>+</sup>Gr1<sup>+</sup>, CD11b<sup>+</sup>Ly6C<sup>+</sup>, and CD11b<sup>+</sup>Ly6G<sup>+</sup> BILs in non-tumor-bearing mice (left), tumor-bearing mice treated with (right) or without (center) celecoxib (*n* = 5/group). The number in each histogram indicates the percentage of double-positive populations. The graph shows the percentages of CD11b<sup>+</sup>Gr1<sup>+</sup> BILs in 3 independent experiments. (B) Expression of *S100A8*, *S100A9*, *SAA3* (*n* = 3/group), and *CCL2* (*n* = 6/group) in the brain of tumor-free mice and tumor-bearing mice treated with or without celecoxib on day 14. (C) Clonogenic assay with mice bearing 4T1 tumors of day 30 treated with or without celecoxib (*n* = 5/group).

This occurred even if the primary tumors were surgically resected (data not shown), and this is consistent with a previous report<sup>31</sup> describing the metastatic activity of 4T1 tumors. The only discrepancy between our

observations and the referenced study is that we observed microscopic brain metastases by day 30 in all mice, while Pulaski and Ostrand-Rosenberg<sup>31</sup> reported that brain metastases were not detected until after day

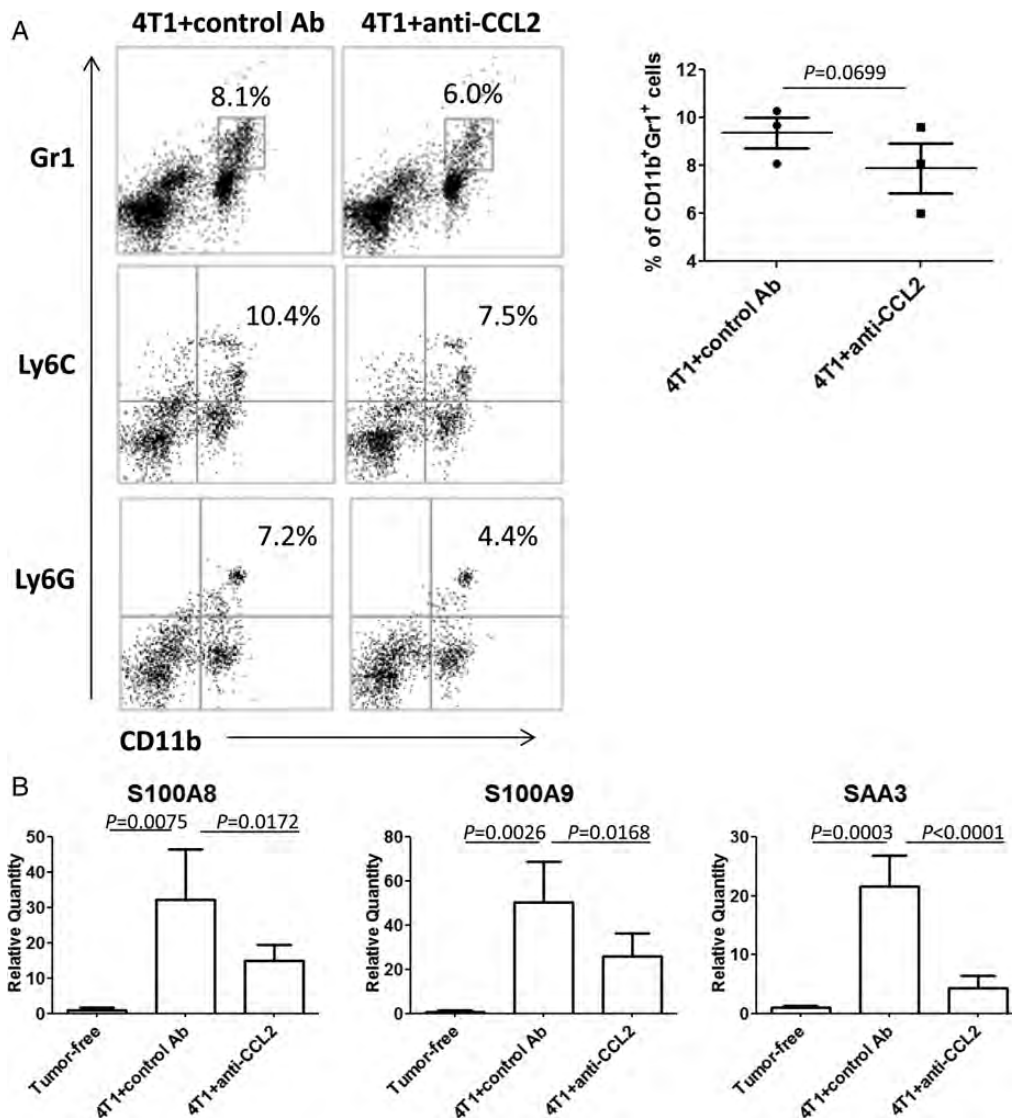


Fig. 6. Anti-CCL2 mAb reduces infiltration of IMCs and expression of *S100A8*, *S100A9*, and *SAA3* in the brain. BALB/c mice bearing 4T1 tumors were treated with anti-CCL2 mAb or control Ab i.p. (A) CD11b<sup>+</sup>Gr1<sup>+</sup>, CD11b<sup>+</sup>Ly6C<sup>+</sup>, and CD11b<sup>+</sup>Ly6G<sup>+</sup> BILs in mice treated with control Ab (left) or with anti-CCL2 mAb (right). The number in each histogram indicates the percentage of double-positive populations. The graph shows the percentages of CD11b<sup>+</sup>Gr1<sup>+</sup> BILs in 3 independent experiments. (B) Expression of *S100A8*, *S100A9*, and *SAA3* in the brain of tumor-free ( $n = 3$ /group) or tumor-bearing mice treated with control IgG or anti-CCL2 mAb ( $n = 6$ /group).

34. This is likely due to the highly sensitive methods that we employed for the detection of brain metastases.

In our data, the liver and the lung of mice bearing 4T1 tumors of day 14 also demonstrated strong trends toward increased CD11b<sup>+</sup>Gr1<sup>+</sup> cell infiltration as well as upregulation of *S100A8/A9*, *SAA3*, and *CCL2* (Supplementary Fig. S2A, C, and D). Systemic administration of celecoxib confirmed the previous observation by Sinha et al.<sup>32</sup> and reduced the number of lung metastases by day 30 (Supplementary Fig. S2B), which was associated with a trend toward suppression of CD11b<sup>+</sup>Gr1<sup>+</sup> cell infiltration and the inflammatory chemokines (Supplementary Fig. S2A, C, and D). Although somewhat less consistently than observed in the brain, treatment with anti-Gr1<sup>+</sup> mAb (Supplementary Fig. S3), anti-S100A9, GB3.1 (Supplementary Fig. S4),

or anti-CCL2 (Supplementary Fig. S5) demonstrated a trend toward reduced accumulation of CD11b<sup>+</sup>Gr1<sup>+</sup> cells in the liver and the lung.

## Discussion

In the current study, we report for the first time that primary breast cancer induces robust inflammatory responses in the brain before tumor cells metastasize (the “premetastatic brain”). COX2/PGE<sub>2</sub> derived from the primary tumor appears to expand BM-derived CD11b<sup>+</sup>Gr1<sup>+</sup> IMCs systemically, including in the brain. SA100A9, which is produced by CD11b<sup>+</sup>Gr1<sup>+</sup> BILs at high levels, attracts BM-derived myeloid cells and 4T1 tumor cells in vitro, suggesting a possibility

that this chemokine pathway promotes further recruitment of CD11b<sup>+</sup>Gr1<sup>+</sup> myeloid cells and tumor cells to the brain. Our data also suggest that depletion of Gr1<sup>+</sup> cells or celecoxib treatment may be useful for prevention of brain metastasis.

Definition of the premetastatic condition required thorough evaluations to prove the absence of tumor cells in the brains of day-14 tumor-bearing mice. To this end, we employed 3 methods: (i) clonogenic assay, (ii) multiphoton microscopic imaging, and (iii) PCR. With these 3 sensitive and complementary methods, we were unable to detect the presence of tumor cells in day-14 brains, while day-30 brains readily showed the presence of tumor cells (Fig. 1). These data provided us with the strong basis to define the premetastatic soil in the brain of mice bearing 4T1 tumors of day 14.

In the current study, the accumulation of BM-derived CD11b<sup>+</sup>Gr1<sup>+</sup> cells in the premetastatic brain was associated with increased expression of *S100A8*, *S100A9*, *SAA3*, and *CCL2* (Fig. 1). Several studies have shown enhanced recruitment of CD11b<sup>+</sup> myeloid progenitor cells in the premetastatic niches and their role in promotion of lung and liver metastases.<sup>23,33,34</sup> Similarly to these previous studies, the lung and the liver of mice bearing 4T1 tumors of day 14 also demonstrated increased CD11b<sup>+</sup>Gr1<sup>+</sup> cell infiltration and upregulation of *S100A8/A9*, *SAA3*, and *CCL2* (Supplementary Fig. S2). Although we did not examine the presence of lung or liver metastases on day 14, according to the previous report,<sup>31</sup> it is highly likely that the metastatic tumors were present in the lung. Previous reports by others using murine lung cancer and melanoma cells have demonstrated that *S100A8*, *S100A9*, and *SAA3* act as positive feedback regulators for the accumulation of myeloid cells and tumor cells in the premetastatic lung.<sup>8,34</sup> Therefore, it is possible that the same mechanisms may operate in the lung metastases of 4T1 tumors in our current model. Further studies are warranted to determine whether the premetastatic inflammatory milieu takes place in the other organs in the 4T1 model. Nonetheless, the current study is the first to demonstrate the premetastatic soil in the brain. As accumulation of CD11b<sup>+</sup>Gr1<sup>+</sup> cells could also be promoted by other pathways, such as CXCL12-CXCR4,<sup>16</sup> further investigations are warranted to understand the precise mechanisms underlying the premetastatic conditioning.

Administration of anti-Gr1 mAb (RB6-8C5) significantly reduced CD11b<sup>+</sup>Gr1<sup>+</sup> cells and tumor metastasis in the brain (Fig. 2). CD11b<sup>+</sup>Gr1<sup>+</sup> myeloid cells are classified as Ly6C<sup>high</sup> or Ly6G<sup>high</sup>, which represent monocytic and granulocytic subpopulations, respectively.<sup>35,36</sup> RB6-8C5 was originally developed to recognize a surface antigen, Gr1,<sup>37</sup> which is a member of the Ly6 gene family. Then, Ly6G was found to be the major antigen detected by RB6-8C5.<sup>38</sup> Hence, RB6-8C5 may preferentially deplete the Ly6G<sup>high</sup> granulocytic subpopulation, which may be responsible for the promotion of brain metastasis. As CD11b<sup>+</sup>Gr1<sup>+</sup> cells are often referred to as myeloid-derived suppressor cells, which are heterogeneous IMCs with potent abilities to suppress T-cell functions,<sup>35</sup> it is possible that the accumulated CD11b<sup>+</sup>Gr1<sup>+</sup> cells promote tumor metastasis by

suppressing antitumor T-cell responses. Further studies are warranted to evaluate this hypothesis.

Although several chemokines, such as *CCL17*, *CCL22*,<sup>14</sup> *CCL28*,<sup>15</sup> *CXCL12*,<sup>16</sup> *CSF-1*,<sup>17</sup> *S100A8*, *S100A9*, and *SAA3*,<sup>8</sup> have been shown to promote tumor metastasis by modulating the immunological environment of the metastatic site, in our model only *S100A8*, *S100A9*, and *SAA3* were upregulated among these chemokines (Fig. 1). Both *S100A8* and *S100A9* belong to the well-conserved S100 family of EF-hand calcium-binding proteins. Activated neutrophils, monocytes, or macrophages as well as CD11b<sup>+</sup>Gr1<sup>+</sup> myeloid cells release these proteins predominantly as *S100A8/A9* heterodimers, which are chemotactic and attract leukocytes in the local microenvironment.<sup>39</sup> Interestingly, the *S100A9*<sup>-/-</sup> mice have no detectable *S100A8* in peripheral blood cells, probably because of higher turnover of isolated *S100A8* in the absence of binding partner *S100A9*.<sup>40</sup> As CD11b<sup>+</sup>Gr1<sup>+</sup> cells were the major producer of *S100A8/A9*, our data in Fig. 3 strongly suggest a role of the positive feedback loop for *S100A8/A9* to promote the accumulation of CD11b<sup>+</sup>Gr1<sup>+</sup> cells and metastasis of 4T1 tumor cells via TLR4. Although systemic treatment with anti-*S100A9* Ab showed a trend toward decreased percentages of CD11b<sup>+</sup>Gr1<sup>+</sup> cell infiltration in the premetastatic brain, the lung, and the liver (Supplementary Fig. S4A and B), the same treatment did not significantly reduce the degree of brain metastasis (data not shown). This may be due to the suboptimal dose of the anti-*S100A9* used in vivo and the contributions of other tumor-derived factors in the promotion of the metastasis. Nonetheless, our data and information from other studies warrant further studies on *S100A9* as an attractive target for prevention of cancer metastasis.

In our study, *SAA3* was one of the most significantly upregulated biological response mediators in the premetastatic brain. *SAA3* is an apolipoprotein and belongs to the family of acute-phase SAA proteins secreted in inflammation.<sup>41</sup> Like *S100A8/A9*, *SAA3* binds to TLR4 and is upregulated in cancer-induced inflammatory conditions.<sup>8</sup> However, although mouse *SAA3* is involved in immune, metabolic, and cardiovascular homeostasis,<sup>42,43</sup> human *SAA3* is encoded by a pseudogene, and its functional protein is not known yet.<sup>41</sup> As such, we consider *SAA3* not highly relevant to humans and therefore focused on *S100A8/A9*. Nonetheless, in mice, *SAA3* was induced by *S100A8/A9* in the premetastatic niche and was able to induce expression of tumor necrosis factor (TNF)- $\alpha$  in macrophages.<sup>44</sup> Conversely, inflammatory cytokines including TNF- $\alpha$  are potent inducers of SAA in macrophages<sup>45</sup> and activate *S100A8/A9*.<sup>46</sup> In our model, upregulation of *S100A8/A9* and *SAA3* in the premetastatic brain was associated with increased serum levels of TNF- $\alpha$  (Supplementary Fig. S6). Hence, in our model, a positive feedback loop of TNF- $\alpha$ , *SAA3*, and *S100A8/A9* may constitute a pro-inflammatory milieu that recruits CD11b<sup>+</sup>Gr1<sup>+</sup> myeloid cells in the brain. Further studies are warranted to determine the specific role of TNF- $\alpha$ .

PGE<sub>2</sub> is an inducer of CD11b<sup>+</sup>Gr1<sup>+</sup> myeloid cells.<sup>32</sup> COX2 expression in primary breast cancer is associated

with metastasis and poor prognosis.<sup>47</sup> Our data using 4T1-COX2 KO cells demonstrated a trend toward reduced formation of brain metastasis compared with the control group (Fig. 4;  $P = .0621$ ). The impact was more striking with celecoxib administration (Fig. 5). This is probably because systemic administration of celecoxib can reduce PGE<sub>2</sub> levels systemically in a variety of cell types, including myeloid cells. Nonetheless, our data using 4T1-COX2 KO cells and JC cells strongly suggest that primary tumor-derived COX2 is still at least partially responsible for the brain metastasis. Taken together, these data indicate that the PGE<sub>2</sub> pathway must play a critical role upstream of the pro-inflammatory milieu, inducing the premetastatic condition in the brain.

The premetastatic condition was also associated with the elevation of CCL2, which is one of the primary chemokines attracting CD11b<sup>+</sup>Gr1<sup>+</sup> myeloid cells.<sup>48</sup> Systemic anti-CCL2 mAb treatment suppressed S100A8/A9 and SAA3 levels (Fig. 6). The trend toward reduced CD11b<sup>+</sup>Gr1<sup>+</sup> BILs by anti-CCL2 mAb treatment did not reach the defined level of significance (Fig. 6A;  $P = .0699$ ). This is likely due to the small-size comparison of results from 3 independent experiments, each of which employed BILs pooled from 3 or 5 mice per group. Nonetheless, since anti-CCL2 mAb treatment significantly reduced S100A8/9 and SAA3 levels (Fig. 6B) and reduced the levels of myeloid cells in lung and liver (Supplementary Fig. S5), it is reasonable to interpret that anti-CCL2 mAb systemically inhibits the inflammatory milieu. Several studies, including ours,<sup>29</sup> have demonstrated the suppression of tumor growth and metastasis through the blockade of myeloid cell accumulation.<sup>30,48</sup> CCL2 blockade also enhanced the efficacy of vaccines against non-small cell lung cancer by enhancing the induction of antigen-specific CD8<sup>+</sup> T-cells and reduction of intratumoral T regulatory cells,<sup>49</sup> supporting future developments of combination approaches using tumor vaccine and CCL2 blockade.

Although the 4T1 tumor model shares many features with human breast cancer in terms of progressive growth in the mammary gland and active metastasis to the draining lymph nodes and other organs,<sup>9,50</sup> one major limitation of the current model may be the short time window for our investigation due to the rapid growth of the tumor, while in humans, it takes at least several years to observe brain metastases. Nonetheless, the key clinical relevance of the current preclinical study is strongly supported by a recent publication demonstrating that daily use of acetylsalicylic acid (also known as aspirin) reduced distant metastases, including brain metastases, in 987 cancer patients.<sup>51</sup> Nonsteroidal anti-inflammatory drugs, including acetylsalicylic acid and celecoxib, mediate their biological effects at least partially by suppression of COX2 and its product PGE<sub>2</sub>, which

in turn induces differentiation of immunoregulatory cells, such as IMCs.<sup>52</sup> Indeed, we recently reported that both acetylsalicylic acid and celecoxib inhibit development of de novo glioma in mice via reduction of IMCs,<sup>11</sup> further supporting the role of COX2-driven IMCs in cancer progression.

Although our data clearly elucidate the roles of some inflammatory mediators that are induced by the primary breast cancer, the concurrent blockade of multiple pathways was found not feasible because administration of multiple mAbs is not well tolerated in tumor-bearing mice (data not shown). Nonetheless, the current study provides us with a strong rationale to evaluate whether S100A9, CCL2, and PGE<sub>2</sub> can serve as biomarkers and therapeutic targets for brain metastasis.

## Supplementary Material

Supplementary material is available online at *Neuro-Oncology* (<http://neuro-oncology.oxfordjournals.org/>).

## Acknowledgments

We thank Drs Yoshiro Maru and Sachie Hiratsuka at Tokyo Women's Medical University for providing us with histidine-fused recombinant murine S100A9 protein. We thank Dr Douglas M. Potter at the University of Pittsburgh for his advice on statistical analyses. A part of the current study was presented at the 16th Annual Scientific Meeting of the Society for Neuro-oncology (Orange County, CA, November 19, 2011) and the 26th Annual Meeting of the Society for Immunotherapy of Cancer (Bethesda, MD, November 5, 2011).

*Conflict of interest statement.* L.A.S. is an employee of Janssen R&D, LLC.

## Funding

This work was supported by the Walter L. Copeland Fund of the Pittsburgh Foundation (Y.L.); the Musella Foundation for Brain Tumor Research and Information (H.O.); the American Brain Tumor Association (A.K.); and the National Institutes of Health (NCI 1P01 CA132714 to H.O., NINDS 2P01 NS40923 to H.O., P30CA047904 for the use of UPCI shared resources: the Animal Facility, the Cell and Tissue Imaging Facility, the Small Animal Imaging Facility, and the Cytometry Facility).

## References

1. Palmieri D, Smith QR, Lockman PR, et al. Brain metastases of breast cancer. *Breast Dis.* 2006;26:139–147.
2. Weil RJ, Palmieri DC, Bronder JL, Stark AM, Steeg PS. Breast cancer metastasis to the central nervous system. *Am J Pathol.* 2005;167(4):913–920.

3. Lin NU, Bellon JR, Winer EP. CNS metastases in breast cancer. *J Clin Oncol*. 2004;22(17):3608–3617.
4. Martin JJ, Kondziolka D. Indications for resection and radiosurgery for brain metastases. *Curr Opin Oncol*. 2005;17(6):584–587.
5. Kondziolka D, Kano H, Harrison GL, et al. Stereotactic radiosurgery as primary and salvage treatment for brain metastases from breast cancer. *J Neurosurg*. 2011;114(3):792–800.
6. Kaplan R, Psaila B, Lyden D. Bone marrow cells in the 'pre-metastatic niche': within bone and beyond. *Cancer Metast Rev*. 2006;25(4):521–529.
7. Maru Y. Logical structures extracted from metastasis experiments. *Cancer Sci*. 2009;100(11):2006–2013.
8. Hiratsuka S, Watanabe A, Sakurai Y, et al. The S100A8-serum amyloid A3-TLR4 paracrine cascade establishes a pre-metastatic phase. *Nat Cell Biol*. 2008;10(11):1349–1355.
9. Pulaski BA, Ostrand-Rosenberg S. Mouse 4T1 Breast Tumor Model. Current Protocols in Immunology. New York: John Wiley & Sons, Inc. 2001.
10. Fujita M, Zhu X, Ueda R, et al. Effective immunotherapy against murine gliomas using type 1 polarizing dendritic cells—significant roles of CXCL10. *Cancer Res*. 2009;69(4):1587–1595.
11. Fujita M, Kohanbash G, Fellows-Mayle W, et al. COX-2 blockade suppresses gliomagenesis by inhibiting myeloid-derived suppressor cells. *Cancer Res*. 2011;71(7):2664–2674.
12. Fujita M, Scheurer ME, Decker SA, et al. Role of type 1 IFNs in anti-glioma immunosurveillance—using mouse studies to guide examination of novel prognostic markers in humans. *Clin Cancer Res*. 2010;16(13):3409–3419.
13. Liu Y, Komohara Y, Domenick N, et al. Expression of antigen processing and presenting molecules in brain metastasis of breast cancer. *Cancer Immunol Immunother*. 2012;61(6):789–801.
14. Olkhanud PB, Baatar D, Bodogai M, et al. Breast cancer lung metastasis requires expression of chemokine receptor CCR4 and regulatory T cells. *Cancer Res*. 2009;69(14):5996–6004.
15. Facciabene A, Peng X, Hagemann IS, et al. Tumour hypoxia promotes tolerance and angiogenesis via CCL28 and Treg cells. *Nature*. 2011;475(7355):226–230.
16. Obermajer N, Muthuswamy R, Odunsi K, Edwards RP, Kalinski P. PGE2-induced CXCL12 production and CXCR4 expression controls the accumulation of human MDSCs in ovarian cancer environment. *Cancer Res*. 2011;71(24):7463–7470.
17. Pyonteck SM, Gadea BB, Wang HW, et al. Deficiency of the macrophage growth factor CSF-1 disrupts pancreatic neuroendocrine tumor development. *Oncogene*. 2012;31(11):1459–1467.
18. Ford AL, Goodsall AL, Hickey WF, Sedgwick JD. Normal adult ramified microglia separated from other central nervous system macrophages by flow cytometric sorting. Phenotypic differences defined and direct ex vivo antigen presentation to myelin basic protein-reactive CD4+ T cells compared. *J Immunol*. 1995;154(9):4309–4321.
19. Eue I, König S, Pior J, Sorg C. S100A8, S100A9 and the S100A8/A9 heterodimer complex specifically bind to human endothelial cells: identification and characterization of ligands for the myeloid-related proteins S100A9 and S100A8/A9 on human dermal microvascular endothelial cell line-1 cells. *Internat Immunol*. 2002;14(3):287–297.
20. Nacken W, Roth J, Sorg C, Kerkhoff C. S100A9/S100A8: Myeloid representatives of the S100 protein family as prominent players in innate immunity. *Microsc Res Tech*. 2003;60(6):569–580.
21. Vogl T, Tenbrock K, Ludwig S, et al. Mrp8 and Mrp14 are endogenous activators of Toll-like receptor 4, promoting lethal, endotoxin-induced shock. *Nat Med*. 2007;13(9):1042–1049.
22. Turovskaya O, Foell D, Sinha P, et al. RAGE, carboxylated glycans and S100A8/A9 play essential roles in colitis-associated carcinogenesis. *Carcinogenesis*. 2008;29(10):2035–2043.
23. Ichikawa M, Williams R, Wang L, Vogl T, Srikrishna G. S100A8/A9 activate key genes and pathways in colon tumor progression. *Mol Cancer Res*. 2011;9(2):133–148.
24. Srikrishna G, Turovskaya O, Shaikh R, et al. Carboxylated glycans mediate colitis through activation of NF- $\kappa$ B. *J Immunol*. 2005;175(8):5412–5422.
25. Ristimäki A, Sivula A, Lundin J, et al. Prognostic significance of elevated cyclooxygenase-2 expression in breast cancer. *Cancer Res*. 2002;62(3):632–635.
26. Capone PM, Kadohama N, Chu TM. Immunotherapy in a spontaneously developed murine mammary carcinoma with syngeneic monoclonal antibody. *Cancer Immunol Immunother*. 1987;25(2):93–99.
27. Chao TY, Chu TM. Characterization of a new spontaneously developed murine mammary adenocarcinoma in syngeneic BALB/c hosts. *In vitro Cell Dev Biol*. 1989;25(7):621–626.
28. Divino CM, Chen SH, Yang W, Thung S, Brower ST, Woo SL. Anti-tumor immunity induced by interleukin-12 gene therapy in a metastatic model of breast cancer is mediated by natural killer cells. *Breast Cancer Res Treat*. 2000;60(2):129–134.
29. Zhu X, Fujita M, Snyder L, Okada H. Systemic delivery of neutralizing antibody targeting CCL2 for glioma therapy. *J Neuro-Onc*. 2011;104(1):83–92.
30. Qian B-Z, Li J, Zhang H, et al. CCL2 recruits inflammatory monocytes to facilitate breast-tumour metastasis. *Nature*. 2011;475(7355):222–225.
31. Pulaski BA, Ostrand-Rosenberg S. Reduction of established spontaneous mammary carcinoma metastases following immunotherapy with major histocompatibility complex class II and B7.1 cell-based tumor vaccines. *Cancer Res*. 1998;58(7):1486–1493.
32. Sinha P, Clements VK, Fulton AM, Ostrand-Rosenberg S. Prostaglandin E2 promotes tumor progression by inducing myeloid-derived suppressor cells. *Cancer Res*. 2007;67(9):4507–4513.
33. Gil-Bernabé AM, Ferjančič Š, Tlalka M, et al. Recruitment of monocytes/macrophages by tissue factor-mediated coagulation is essential for metastatic cell survival and premetastatic niche establishment in mice. *Blood*. 2012;119(13):3164–3175.
34. Hiratsuka S, Watanabe A, Aburatani H, Maru Y. Tumour-mediated upregulation of chemoattractants and recruitment of myeloid cells pre-determines lung metastasis. *Nat Cell Biol*. 2006;8(12):1369–1375.
35. Gabrilovich DI, Ostrand-Rosenberg S, Bronte V. Coordinated regulation of myeloid cells by tumours. *Nat Rev Immunol*. 2012;12(4):253–268.
36. Ostrand-Rosenberg S. Myeloid-derived suppressor cells: more mechanisms for inhibiting antitumor immunity. *Cancer Immunol Immunother*. 2010;59(10):1593–1600.
37. Tepper RI, Coffman RL, Leder P. An eosinophil-dependent mechanism for the antitumor effect of interleukin-4. *Science*. 1992;257(5069):548–551.
38. Fleming T, Fleming M, Malek T. Selective expression of Ly-6G on myeloid lineage cells in mouse bone marrow. RB6–8C5 mAb to granulocyte-differentiation antigen (Gr-1) detects members of the Ly-6 family. *J Immunol*. 1993;151(5):2399–2408.
39. Sinha P, Okoro C, Foell D, Freeze HH, Ostrand-Rosenberg S, Srikrishna G. Proinflammatory S100 proteins regulate the accumulation of myeloid-derived suppressor cells. *J Immunol*. 2008;181(7):4666–4675.
40. Manitz M-P, Horst B, Seeliger S, et al. Loss of S100A9 (MRP14) results in reduced interleukin-8-induced CD11b surface expression, a polarized microfilament system, and diminished responsiveness to chemoattractants in vitro. *Mol Cell Biol*. 2003;23(3):1034–1043.

41. Gomez R, Conde J, Scotece M, Gomez-Reino JJ, Lago F, Gualillo O. What's new in our understanding of the role of adipokines in rheumatic diseases? *Nat Rev Rheumatol*. 2011;7(9):528–536.
42. Pickup J, Mattock M, Chusney G, Burt D. NIDDM as a disease of the innate immune system: association of acute-phase reactants and interleukin-6 with metabolic syndrome X. *Diabetologia*. 1997;40(11):1286–1292.
43. Han CY, Subramanian S, Chan CK, et al. Adipocyte-derived serum amyloid A3 and hyaluronan play a role in monocyte recruitment and adhesion. *Diabetes*. 2007;56(9):2260–2273.
44. Tomita T, Sakurai Y, Ishibashi S, Maru Y. Imbalance of Clara cell–mediated homeostatic inflammation is involved in lung metastasis. *Oncogene*. 2011;30(31):3429–3439.
45. Son D-S, Roby KF, Terranova PF. Tumor necrosis factor- $\alpha$  induces serum amyloid A3 in mouse granulosa cells. *Endocrinology*. 2004;145(5):2245–2252.
46. Xu K, Geczy CL. IFN- $\gamma$  and TNF regulate macrophage expression of the chemotactic S100 protein S100A8. *J Immunol*. 2000;164(9):4916–4923.
47. Lucci A, Krishnamurthy S, Singh B, et al. Cyclooxygenase-2 expression in primary breast cancers predicts dissemination of cancer cells to the bone marrow. *Breast Cancer Res Treat*. 2009;117(1):61–68.
48. Huang B, Lei Z, Zhao J, et al. CCL2/CCR2 pathway mediates recruitment of myeloid suppressor cells to cancers. *Cancer Lett*. 2007;252(1):86–92.
49. Fridlender ZG, Buchlis G, Kapoor V, et al. CCL2 blockade augments cancer immunotherapy. *Cancer Res*. 2010;70(1):109–118.
50. Sinha P, Clements V, Miller S, Ostrand-Rosenberg S. Tumor immunity: a balancing act between T cell activation, macrophage activation and tumor-induced immune suppression. *Cancer Immunol Immunother*. 2005;54(11):1137–1142.
51. Rothwell PM, Wilson M, Price JF, Belch JFF, Meade TW, Mehta Z. Effect of daily aspirin on risk of cancer metastasis: a study of incident cancers during randomised controlled trials. *Lancet*. 2012;379(9826):1591–1601.
52. Wang D, Dubois RN. Eicosanoids and cancer. *Nat Rev Cancer*. 2010;10(3):181–193.